ЖУРНАЛ ВЫСШЕЙ НЕРВНОЙ ДЕЯТЕЛЬНОСТИ, 2024, том 74, № 3, с. 336–352

ФИЗИОЛОГИЧЕСКИЕ МЕХАНИЗМЫ ПОВЕДЕНИЯ ЖИВОТНЫХ: ВОСПРИЯТИЕ ВНЕШНИХ СТИМУЛОВ, ДВИГАТЕЛЬНАЯ АКТИВНОСТЬ, ОБУЧЕНИЕ И ПАМЯТЬ

УДК 612.82:004.032.26: 796.015.576; 577.175.82: 612.181.5

HYPOXIC PRECONDITIONING IN RATS WITH LOW AND HIGH PREPULSE INHIBITION OF ACOUSTIC STARTLE IS IMPLEMENTED THROUGH TOPOGRAPHICALLY DIFFERENT SENSORY INPUTS. WORKING HYPOTHESIS

© 2024 г. E. I. Zakharova[a, #], Z. I. Storozheva[b], A. T. Proshin[b], M. Yu. Monakov[a], A. M. Dudchenko[a]

[a] *Institute of General Pathology and Pathophysiology, Moscow, Russia*

[b] *Federal Research Center for Original and Promising Biomedical and Pharmaceutical Technologies, Moscow, Russia*

 # e-mail: zakharova-ei@yandex.ru

Received November 27, 2023; Revised February 08, 2024; Accepted March 11, 2024

The neurotransmitter and network mechanisms of hypoxic preconditioning are practically unknown. Previously, in rats, we identified the key role of the hippocampus and its cholinergic projections in the preconditioning mechanism of single-exposure of moderate hypobaric hypoxia (HBH) based on the association between the efficiency of HBH and the magnitude of Prepulse Inhibition of Acoustic Startle (PPI). This study presents the first data on PPI-dependent neuronal networks of hypoxic preconditioning and their cholinergic components. The activity of synaptic choline acetyltransferase (ChAT), an indicator of cholinergic function, was used for a correlation analysis of ChAT response to HBH in the hippocampus, cerebral cortex, and caudal brainstem in animals with different levels of PPI. In rats with PPI < 40%, ChAT activity was correlated in the hippocampus, cortex and caudal brainstem, while in rats with PPI > 40% in the hippocampus and cortex. It is hypothesized that HBH is realized through topographically different sensory inputs, namely through respiratory neurons of the brainstem in rats with low PPI and respiratory neurons of the olfactory epithelium in rats with high PPI.

Keywords: hypoxic preconditioning; neuronal/ neural networks; HBH; PPI; hippocampus; cerebral cortex; caudal brainstem; cholinergic forebrain projective neurons and interneurons; 'light' and 'heavy' synaptosomes; synaptic membrane-bound and soluble ChAT

DOI: 10.31857/S0044467724030074

INTRODUCTION

Changes in the oxygen content of the inhaled air can have both positive and negative effects on the aerobic organism. This depends on the depth of oxygen deficiency and the length of stay in such conditions (Navarrete-Opazo, Mitchell, 2014; Ando et al., 2020).

Moderate hypoxia is a necessary natural factor in cellular differentiation and proliferation at different stages of prenatal ontogenesis (Radhakrishnan et al., 2021). This suggests the presence of genetic and metabolic pathways of cell adaptation to hypoxic influences in all body tissues and explains the phenomenon of the 'cross-adaptation' of hypoxic training to damaging factors of other origins (Rybnikova, Zenko, 2019).

That's why treatment of the body or individual organs with an adaptive, moderately reduced concentration of oxygen in the air in courses (interval) or in short-term one-day hypoxic training (hypoxic preconditioning) can increase the resistance of organs and tissues to the damaging effects of severe hypoxic or ischemic strokes (Das, Das, 2008; Gavrilova et al., 2008; Lukyanova et al., 2008, 2009; Maslov et al., 2011; Rybnikova et al., 2022).

It is known that the brain is the most sensitive organ to hypoxia (Akopyan et al., 1984; Maslov et al., 2011; Liu et al., 2022) and the brain is a leading regulatory system in all body functions. The central nervous system is realized through the neural networks. Currently, the question of the neural networks of cognitive functions is being actively examined, and this includes investigations of synaptic plasticity (Obermayer et al., 2019; Appelbaum et al., 2022; Lara-González et al., 2022). At the same time, the neuronal, including the synaptic organization of hypoxic adaptation functions remains poorly understood.

Our studies on the one-time moderate hypobaric hypoxia model (HBH) allowed us to analyze the central cholinergic systems in the neuronal organization of hypoxic preconditioning.

In rats, HBH (5000 m, pO_2 is 85 mm Hg, 60 min) initiates a most pronounced preconditioning effect in the first minutes of reoxygenation that provides increased resistance to severe hypobaric hypoxia, in-

compatible with life (SHBH, 11500 m, pO_2 is 31 mm Hg) (Lukyanova et al., 2008, 2009). Using the same hypoxic regime, we confirmed the pronounced preconditioning effect of HBH after 4 min of reoxygenation (Zakharova et al., 2011; Zakharova, Dudchenko, 2016). By using the HBH-SHBH test, we found that the efficiency of HBH was associated with the efficiency of sensory-motor gating estimated by the magnitude of Prepulse Inhibition of Acoustic Startle (PPI). The values of HBH efficiency were inversely proportional to the PPI values (Dudchenko et al., 2014). All subsequent experiments confirmed this regularity (Zakharova et al., 2018a, 2018b, 2020). This allowed us to investigate the preconditioning mechanisms of HBH by using the PPI test readings as a predictor of the efficiency of hypoxic training.

By studying the cholinergic brain system in the mechanism of HBH, we identified the following regularities:

(1) Administration of cholinergic ligands PNU-282987 (PNU), a selective agonist of alpha7 subtype of nicotinic receptor (nAChR), and dimethyl sulfoxide (DMSO), an anti-acetylcholinesterase agent at a concentration of 2–3% (Sawada, Sato, 1975), had the multidirectional effects on the efficiency of HBH in rats with PPI greater and less than 40%. The results suggest the involvement of the cholinergic system in the preconditioning mechanism of HBH and the existence of at least two cholinergic mechanisms (Zakharova et al., 20218a, 2018b, 2020).

(2) Choline acetyltransferase (ChAT, acetyl-CoA: choline O-acetyl transferase, EC 2.3.1.6) is a marker of cholinergic neurons and the most specific indicator for monitoring the functional state of cholinergic neurons (Monmaur et al., 1984; Dunbar et al., 1993; Zakharova, Dudchenko, 2014; Bagwe, Sathaye, 2022; Kirstein et al., 2022; AlQot, Rylett, 2023). We measured ChAT activity in the synaptic membranes (membrane-bound ChAT, mChAT) and synaptoplasm (water-soluble ChAT, sChAT) subfractions. This made it possible to identify mChAT, whose activity is a minor part of the total synaptic ChAT (Zakharova, Dudchenko, 2014).

Under HBH, synaptic mChAT changed its own activity in different directions in subgroups of rats with PPI greater and less than 40%. This was observed in only the hippocampus, but not in the caudal brainstem or cerebral cortex (Zakharova et al., 2020). The biochemical data coincided with the results of our pharmacological study and allowed us to assume that the hippocampus is crucial for the preconditioning effect of HBH.

(3) The hippocampus hypothesis was confirmed in our pharmacological study with the intrahippocampal administration of cholinergic ligands in rats with PPI > 40% (Zakharova et al., 2021).

(4) Multidirectional changes in the mChAT activity were observed selectively in the light fraction of hippocampal synaptosomes, in which the presynapses of cholinergic projections from forebrain nuclei are concentrated (Zakharova, Dudchenko, 2014). Thus, we have clarified that a key role in the mechanisms of hypoxic preconditioning is played by the hippocampal cholinergic projections.

(5) In the brain cortex and caudal brainstem, the synaptic ChAT response to HBH did not agree with our pharmacological data. At the same time, the caudal brainstem is a primary sensor of vegetative information, including respiratory signals ('the primary respiratory network') (Ashhad et al., 2022; Karalis, Sirota, 2022) and the cortex is a structure, in which the processing of sensory information preceded that in the hippocampus (Yang et al., 2021; Karalis, Sirota, 2022). This suggested the involvement of these brain structures in hypoxic preconditioning neuronal networks.

To identify HBH-initiated interstructural connections, in this study, a correlation analysis of biochemical parameters of the hippocampus, cerebral cortex and caudal brainstem was carried out. The activity of mChAT, sChAT and the content of membrane and synaptoplasmic proteins (Pr, mPr and sPr) in subfractions of synaptic membranes and synaptoplasm isolated from light and heavy synaptosomes of each brain structure were analyzed.

In the models of hypoxic preconditioning, the cholinergic components of neuronal network in the mechanisms of their protective action have not yet been studied, especially taking into account the dependence of these mechanisms on the PPI value. Thus, the proposed study is the first in this scientific direction.

The main purpose of the study was to determine whether there are connections between HBH-initiated cholinergic changes in the hippocampus, caudal brainstem and cerebral cortex, and the specificity of these connections in rats with PPI < 40% and PPI > 40%?

METHODS

The behavioral experiments were carried out in male albino laboratory outbred rats that were aged 2.5–3.5 months (250–350 g). The animals came from the Light Mountains Nursery (Moscow region, Rus-

sia) and were kept in the vivarium of the Institute of General Pathology and Pathophysiology. The number and suffering of the experimental animals has been minimized. The rats were housed in a temperature-controlled room (20–24 °C) and were exposed to a 12 h light–dark cycle. They were kept with 5–7 animals per rat cage with a size of 40 × 60 cm, and they had free access to food and water. All animal care and experimental procedures were carried out in accordance with EU Directive 2010/63/EU. All experimental protocols were approved by the Ethical Committee of the Institute of General Pathology and Pathophysiology. After the behavioral experiments, the rats were selected for the biochemical experiment.

Acoustic startle reaction model

The acoustic sensorimotor startle reaction model (PPI Test) (Wood et al., 1998) was measured by using a startle response system (TSE System, Bad Homburg, Germany) as previously described (Zakharova et al., 2021).

Rats were tested in soundproof boxes within restraining metal cages that were installed on a platform (27 × 9 × 19 cm). The acoustic stimuli were issued from two loudspeakers, which were mounted on the walls of the metal cages. Broadband noise with duration of 100 ms and a loudness of 110 dB was used as the main stimulus. The background-masking sound signal had broadband noise with a loudness of 72 dB, and the prestimulus (prepulse) had signal duration of 40 ms and a loudness of 85 dB. The animals were exposed to a total of 12 trials after 5 min of adaption. The first two trials were pulse-only trials (habituation). The remaining 10 trials were presented in a pseudo-random order and included five pulse-only trials and five pulse trials with a preceding prepulse of 100 ms in a lead-off interval. The intertrial intervals had a mean value of 15 s (from 10 to 20 s). The PPI value was estimated by using the formula (Am − Ap)/Am × 100%, where Am is the average reaction amplitude in the samples without a prepulse, excluding the first two (n = 5), and Ap is the average reaction amplitude in the samples with a prepulse (n = 5).

Hypoxic preconditioning model

The HBH and SHBH models were used as previously described (Zakharova, Dudchenko 2016; Zakharova et al., 2020).

In the HBH model, a pressure chamber was used for the simultaneous testing of few rats (a branded pressure chamber from "Schrödeu.Co", Germany). The chamber was connected to a single-stage vacuum pump (model VP 115, 2016, YANG YI, China) and an altitude gauge, which was calibrated to an altitude above sea level (model VD-20, # 152300254, 2016, RF). The rats in the chamber were "raised" at a speed of 12–15 m/s to the adaptive altitude of 5000 m (pO_2 is 85 mm Hg, equivalent to 11% O_2, 60 min) and "descended" at the same speed at the end of the training.

In the SHBH model, pressure chambers were used to test one rat in each of them. Each chamber is equipped with a vacuum cap with a needle valve and valves for a vacuum pump and altimeter inlets. The rat was "raised" at a speed of 63.5–64 m/s to the critical altitude of 11.500 m (pO_2 is 31 mm Hg, equivalent to 4.5% O_2). In the critical altitude test, the resistance to hypoxia was recorded as the time (T) until agonal inspiration (apnoea) in combination with a loss of control of body tone. When these symptoms were achieved, the animal immediately "descended" using wide access of atmospheric air into the chamber.

Preparative and Biochemical procedures

The methods of preparation of the synaptosomal subfractions from the brain tissue structures and the determination of the ChAT activity and protein content were the same as previously described (Zakharova et al., 2020, 2022).

The preparative procedures were performed at 2–4 C°. The hippocampus, cerebral cortex, and caudal brainstem (medulla oblongata + pons Varolii) were separated from a brain. From each structure, the light and heavy fractions of synaptosomes were obtained from the rough mitochondrial fraction. The synaptosomal fractions were precipitated and disrupted. From each disrupted synaptosomal fraction, the subfractions of synaptoplasm and synaptic membranes were obtained. All samples were stored at -80 °C.

The ChAT activity was determined by using Fonnum's radiometric method (Fonnum, 1969). The protein content was measured by using Lowry's spectrophotometric method (Lowry et al., 1959).

Experimental Protocol

The rats were handled for at least two consecutive days before starting the experimental procedures.

All experimental rats (n = 60) were tested with the acoustic sensorimotor startle reaction model (PPI model), and the values of PPI were estimated. After that, the rats were subdivided into the control group (n = 6) and HBH group (n = 6). As far as possible, for the control and HBH groups, the rats with the lowest and highest PPI values were taken to more clearly identify the biochemical correlates of the PPI-associated values. PPI values were, respectively, -4.4, +11.9, +29.8

and -1.1, +19.2, +37.5 for the control and HBH rats in the subgroups with PPI < 40% and + 68.0, +87.2, +91.7 and +64.3, +83.9, +93.2 for the control and HBH rats in the subgroups with PPI > 40%.

Several days after the PPI testing, the rats were subjected to subsequent experimental procedures.

The rats in the HBH group were subjected to an HBH session; 4 min after it ended, they were taken for an acute biochemical experiment. The first minutes of reoxygenation after HBH had the most pronounced preconditioning effect (Das, Das, 2008; Lukyanova et al., 2008, 2009), and we selected 4 min as the optimal time period for our experimental conditions. The animals in the control group were taken directly for the biochemical experiment, bypassing HBH.

In the same HBH regime, rats were tested for resistance to SHBH ('HBH + SHBH' group). Intact rats ('SHBH' group) served as controls. Animals within a similar range of PPI values were selected into both SHBH groups. PPI values were, respectively, from −13.1% to +36.6 (n = 13) and from -12.2% to +37.8 (n = 11) for the 'SHBH' and 'HBH + SHBH' rats in the subgroups with PPI < 40% and from +38.3% to +92.5% (n = 11) and from +39.6% to +91.1 (n = 10) for the 'SHBH' and 'HBH + SHBH' rats subgroups with PPI > 40%.

The activity of ChAT and the protein content was determined in the subfractions of the synaptic membranes and synaptoplasm of light and heavy synaptosomes isolated from the cortex, hippocampus, and caudal brainstem. Thus, the membrane-bound mChAT activity and mPr content were estimated in the synaptic membrane subfractions, while the water-soluble sChAT activity and sPr content were estimated in the synaptoplasm subfractions.

All data were obtained in a blind manner. The experimenters did not know the key characteristics of tested rats at the stage of obtaining experimental data; the experiments and animal preparation were performed by different experimenters.

Statistics

The results of the biochemical experiments were expressed in units of ChAT activity per minute or units of protein content in 1 g of raw tissue from a corresponding brain structure.

The normality of all data was assessed with STATISTICA 8.0 (StatSoft Inc. USA) by using the Kolmogorov–Smirnov test (parameter d and *p*-values). No deviations from normality were found.

The results were statistically processed with STATISTICA 8.0 (StatSoft Inc. USA) by using the non-parametric Fisher's exact test (FET criterion) and/ or Wilcoxon-Mann-Whitney test (u-criterion). A correlation analysis was performed by using Pearson's *r*-criterion in Microsoft Excel, and a correcting formula was used for small samples where $n \leqslant 15$ (Kobzar, 2006). For correlation analysis, the variation samples included the values of the corresponding control and HBH subgroups, n = 6 for each sample. The differences and correlations were considered significant at $p < 0.05$.

RESULTS

Resistance to SHBH in the PPI-Associated Subgroups of Rats under the Control and HBH Conditions

The control rats ('SHBH' group) exposed to direct SHBH showed a usual spectrum of innate resistance to severe hypoxia from 37 s to 1289 s in a PPI-independent manner. Average T values (M ± m) were, respectively, 344 ± 89 s (n = 13) and 362 ± 91 s (n = 11) for the 'SHBH' rats in the subgroups with PPI < 40% and PPI > 40%. T-PPI values were not correlated (in the general data array, r = -0.098, n = 24, P > 0.05).

In the 'HBH + SHBH' group, Average T values were, respectively, 802 ± 72 s (n = 11) and 656 ± 63 s (n = 10) for the rats in the subgroups with PPI less and greater than 40%. HBH increased resistance to SHBH by 2.4 times in rats with PPI < 40% (P < 0.001) and by 1.8 times in rats with PPI > 40% (P < 0.005). T-PPI values were correlated (in the general data array, r = -0.594, P < 0.01, n = 21).

Synaptic ChAT Activity and Protein Content in the PPI-Associated Subgroups under the Control and HBH Conditions

The values of synaptic ChAT activity and protein content in the control and HBH subgroups of rats with PPI < 40% and > 40% are shown in Figures 1 and 2, respectively. These data formed the basis for the correlation analysis.

The main results on ChAT activity were published and discussed in detail previously (Zakharova et al., 2020). Here we present new data on protein content, as well as data on ChAT activity in a new format.

The ChAT activity was present in natural quantities (Figure 1). This made it possible to demonstrate the PPI-associated features of the enzyme's reaction to HBH. It can be seen that reciprocal changes in ChAT (mChAT) activity were observed only in the hippocampus and in the subfraction of synaptic

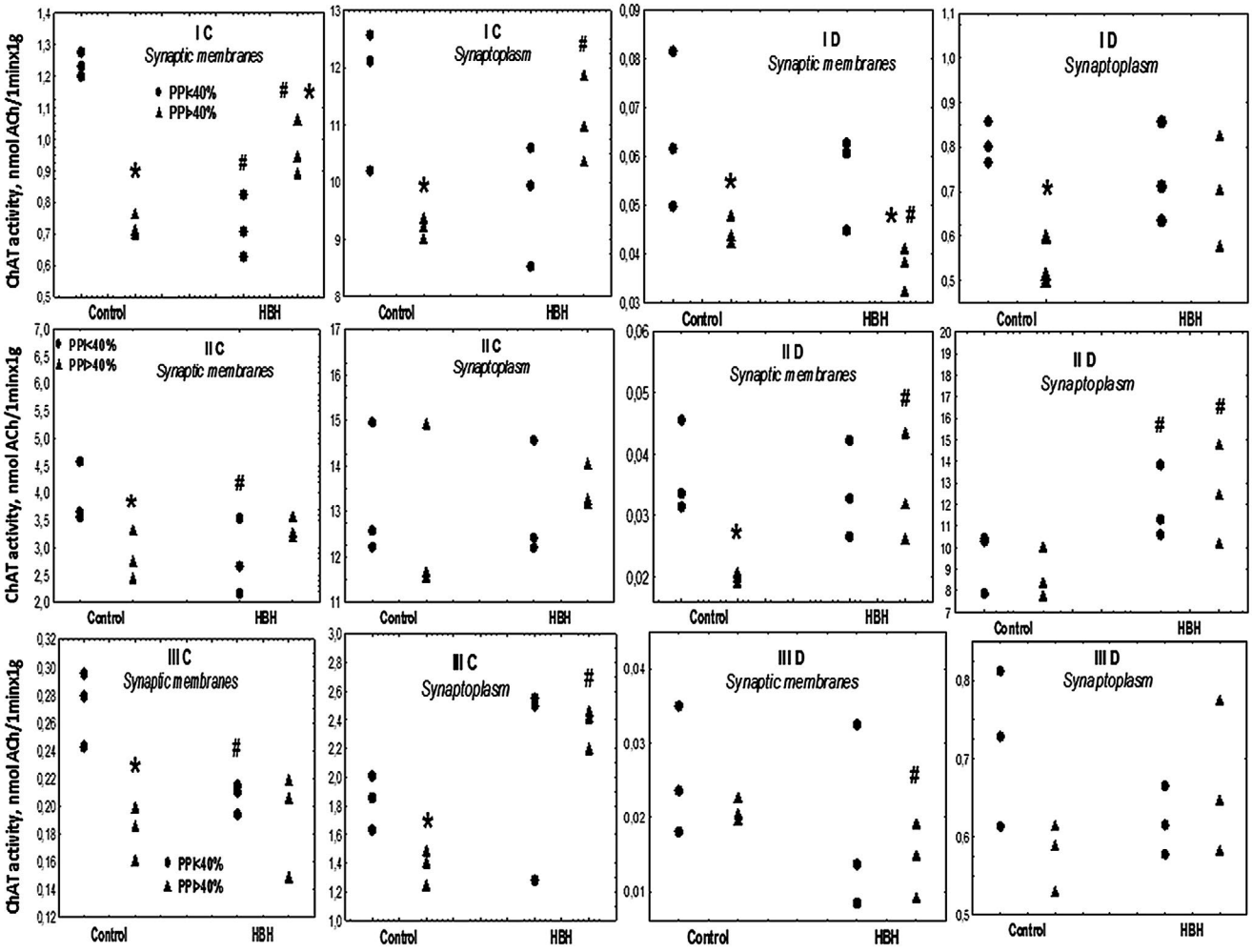

Fig. 1. Individual values of the synaptic ChAT activity in the control and HBH subgroups of rats with PPI values of <40% and >40%. Designations. The ChAT activity is presented in nmol ACh/1 min in 1 g wet weight of the corresponding brain structure. The software package STATISTICA 8.0 (StatSoft., USA) was used to visualize the data. I, hippocampus; II, cerebral cortex; III, caudal brainstem. C, the fraction of light synaptosomes. D, the fraction of heavy synaptosomes. Synaptic membranes, the subfraction of synaptic membranes. Synaptoplasm, the subfraction of the synaptoplasm. Control, the control subgroups of rats. HBH, the subgroups of rats after one-time moderate hypobaric hypoxia (85 mm Hg, equivalent to 11% O_2, 60 min). N = 3 for each subgroup. *, the significant differences in ChAT activity values between the paired subfractions of rats with PPI < 40% and PPI > 40%, $p < 0.05$. #, the significant changes in the ChAT activity values after HBH were compared with the corresponding control subgroup, $p < 0.05$. Fisher's exact test (FET criterion).

Рис. 1. Индивидуальные значения синаптической активности ХАТ в контрольной и НВН подгруппах крыс со значениями ПСТ < 40% и > 40%. Обозначения. Активность ХАТ представлена в нмоль АХ/1 мин в 1 г сырой массы соответствующей структуры мозга. Для визуализации данных использовали пакет программ STATISTICA 8.0 (StatSoft., США). I – гиппокамп; II – кора головного мозга; III – каудальный ствол головного мозга (продолговатый мозг + Варолиев мост). C – фракция легких синаптосом. D – фракция тяжелых синаптосом. Synaptic membranes –субфракция синаптических мембран. Synaptoplasm – субфракция синаптоплазмы. Control – контрольные подгруппы крыс. НВН — подгруппы крыс после однократной умеренной гипобарической гипоксии (85 мм рт. ст., эквивалентно 11% O_2, 60 мин). N = 3 для каждой подгруппы. * – достоверные различия в активности ХАТ между субфракциями у крыс с ПСТ < 40% и ПСТ > 40% в пределах подгруппы, $p < 0.05$. # – достоверные изменения в активности ХАТ после ГБГ по сравнению с соответствующей контрольной подгруппой, $p < 0.05$. Точный Метод Фишера (ТМФ-критерий).

membranes in the light fraction of synaptosomes. In most other subfractions, the ChAT response to HBH was manifested in one of the subgroups or the changes in ChAT activity were unidirectional (in the synaptoplasm subfraction in the heavy synaptosomes of the cerebral cortex).

As a result, under the influence of HBH, the vector of differences in the mChAT activity in the light synaptosomes of the hippocampus significantly changed to the opposite value. In the remaining subfractions, there was an alignment of the initial, control differences in ChAT values between the

subgroups. The exception to the latter pattern was the heavy hippocampal synaptosomes, in which, due to a drop in mChAT activity in the subgroup of rats with PPI > 40%, the differences in enzyme activity observed in the control subgroups became even more pronounced under the influence of HBH.

The results revealed by protein content replicate changes in ChAT activity in response to HBH in a number of subfractions in both subgroups of rats, and also exhibit a response independent of the response of ChAT activity to HBH (in subfractions D of the hippocampus in rats with PPI < 40%), (Figure 2). We will present the results of the ChAT-Pr correlation analysis below.

Conjugacy of HBH-initiated Changes in the Synaptic ChAT activity and Protein Content in the Hippocampus, Cerebral Cortex, and Caudal Brainstem in the Subgroups of Rats with PPI values of < 40% or > 40%

To perform correlation analysis of biochemical parameters, we included data on HBH and the corresponding control in each sample (n = 6). This made it possible to identify the consistency of the response of identical indicators to hypoxia in different brain structures, as well as different indicators within the synaptosomal fraction (ChAT-Pr, mChAT-sChAT and mPr-sPr correlations).

Subgroup of Rats with PPI < 40%

In the subgroup of rats with PPI < 40%, a decrease in ChAT activity and Pr content prevailed (Figure 3,

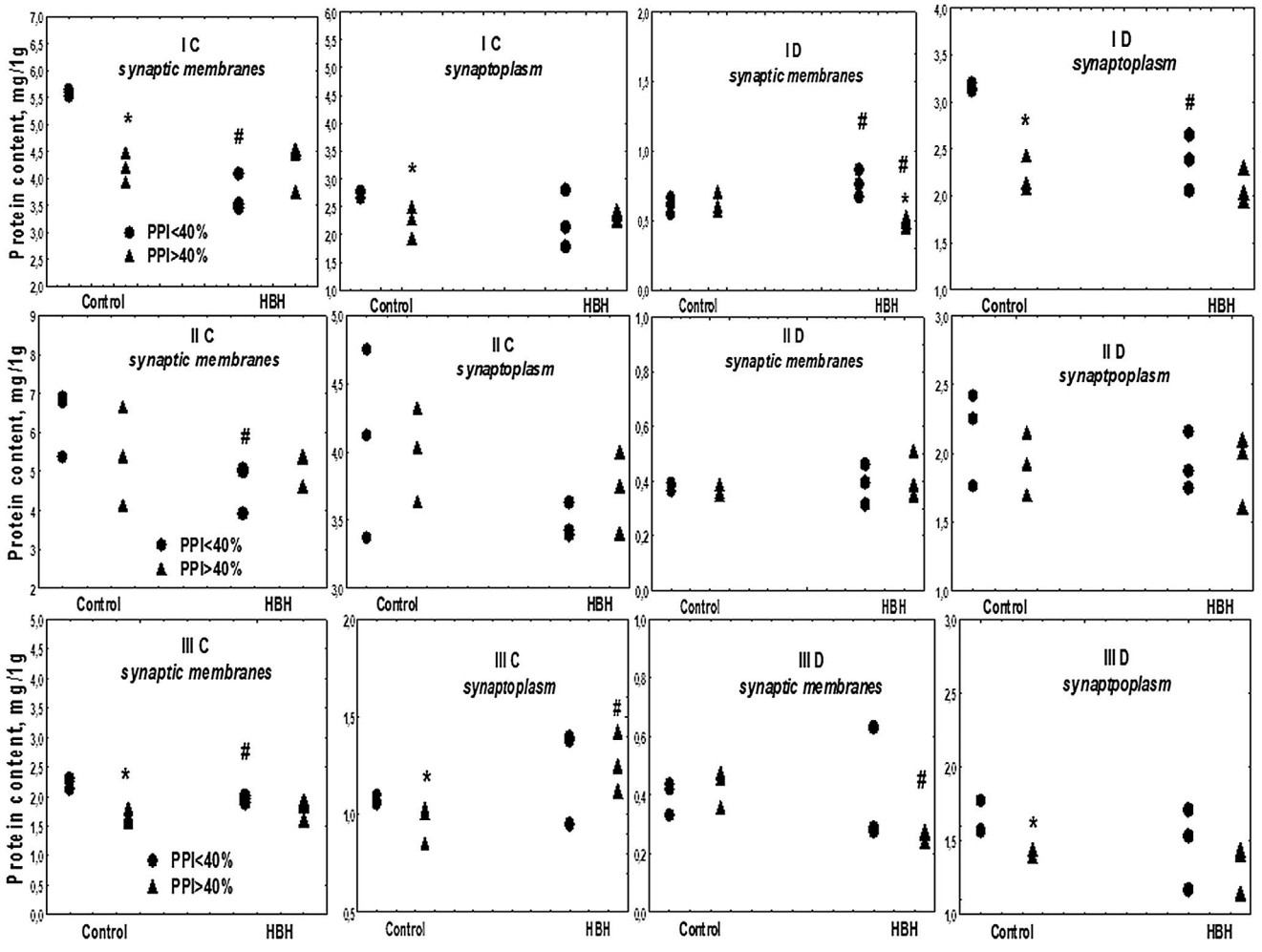

Fig. 2. Individual values of the protein content in the control and HBH subgroups of rats with PPI values of <40% and >40%. Designations. The protein content is presented in mg in 1 g wet weight of the corresponding brain structure.The remaining designations are the same as those in Figure 1.

Рис. 2. Индивидуальные значения содержания белка в контрольной и НВН подгруппах крыс со значениями ПСТ<40% и >40%. Обозначения. Содержание белка представлено в мг в 1 г сырой массы соответствующей структуры мозга. Остальные обозначения как на рис. 1.

Table 1, I – III). A positive correlation was observed between changes in mChAT activity and in mPr content between the fractions of light synaptosomes of the caudal brainstem and hippocampus, as well as between the caudal brainstem and cerebral cortex. In all three fractions, the decrease in mPr content was associated with a decrease in mChAT activity. When comparing the mChAT–mChAT and mPr–mPr values in these fractions between the hippocampus and cerebral cortex, there was no conjugacy of changes.

In addition, HBH initiated the changes in Pr content that did not depend on the cholinergic index: an increase in mPr and a decrease in sPr in the heavy fraction of the hippocampal synaptosomes. The increase in mPr content was negatively correlated with the decrease in mPr content in the light fraction of the hippocampus, and the decrease in sPr content was positively correlated with the decrease in mPr content in the light fractions of both the hippocampus and caudal brainstem.

Subgroup of Rats with PPI > 40%

In the subgroup of rats with PPI > 40%, after HBH, ChAT activation prevailed without changes in the Pr content (Figure 4, Table 1, IV – VI).

The following interstructural associations of ChAT activity were identified: (1) a positive correlation between the activation of mChAT in the light fraction of hippocampal synaptosomes and mChAT in the heavy fraction of cortical synaptosomes; (2) a negative correlation between the inhibition of mChAT in the heavy fraction of the hippocampus and the activation of sChAT in the heavy fraction of the cerebral cortex; (3) a positive correlation of the sChAT activation in the light fraction of the hippocampus with the sChAT activation in the light fraction of the caudal brainstem and, simultaneously, a negative correlation with the inhibition of mChAT in the heavy fraction of the caudal brainstem.

An increase in sPr content was associated with an increase in sChAT activity only in the light fraction of synaptosomes of the caudal brainstem. In addition, the increased sPr content in this fraction turned out to be negatively correlated with a decrease in mPr content in the heavy fraction of the hippocampus. In the heavy fractions of the hippocampus and caudal brainstem, the values of both cholinergic and protein s-indicators decreased, but no significant intrastructural correlations were found.

DISCUSSION

In the rats of 'HBH + SHBH' group tested at the critical altitude, HBH significantly increased SHBH tolerance (T values) in a PPI-dependent manner, averaging 2.4- and 1.8-fold in the subgroups with PPI less than and greater than 40%, respectively. In the 'HBH + SHBH' group, a significant T-PPI dependence was observed, in contrast to the SHBH control group. Data on all characteristics are fully consistent with those obtained previously (Dudchenko et al., 2014; Zakharova, Dudchenko, 2016; Zakharova et al., 2018a, 2018b, 2020).

Our study revealed for the first time a number of related changes in the synaptic ChAT activity and Pr content in the cerebral cortex, hippocampus and caudal brainstem under HBH conditions.

The presynapses of cholinergic projections of the hippocampus and cerebral cortex were mainly concentrated in the light fractions of synaptosomes and the presynapses of cholinergic interneurons in the heavy fraction of synaptosomes (see the review in (Zakharova, Dudchenko, 2014)).

Only the light synaptosomes of the hippocampus were a fraction whose cholinergic presynapses responded to HBH with multidirectional changes in ChAT activity. This cholinergic reaction corresponded to the division of rats into subgroups at the boundary of approximately 40% PPI in our pharmacological data. Activation of cholinergic mediator function by DMSO reduced the preconditioning effect of HBH on resistance to SHBH in rats with PPI < 40% in IP administration and potentiated it in rats with PPI > 40% in IP and intrahippocampal administration (Zakharova et al., 2020, 2021, 2022).

From this it followed that the hippocampus is a key structure in the mechanisms of hypoxic preconditioning, namely, its cholinergic projections from the corresponding forebrain nuclei (Figure 5).

Participation of the hippocampal cholinergic projections in generation of the hippocampal theta rhythm in response to significant stimuli of any modality is known (Kitchigina, 2004; Yoder, Pang, 2005). In the electrophysiological studies, an increase in the power of slow wave activity in the EEG spectrum is a stable symptom of moderate brain hypoxia in a wide range of its values, starting at an altitude of 2000 m (pO2 is 125 mm Hg). This has been shown in both rodent and human brains, and all publications mention the theta rhythm (Akopyan et al., 1984; Ramadan et al., 2020).

Therefore, when analyzing interstructural correlations, we took into account coherence with mChAT activity in the presynapses of light synaptosomes of the hippocampus as the elements of neural network

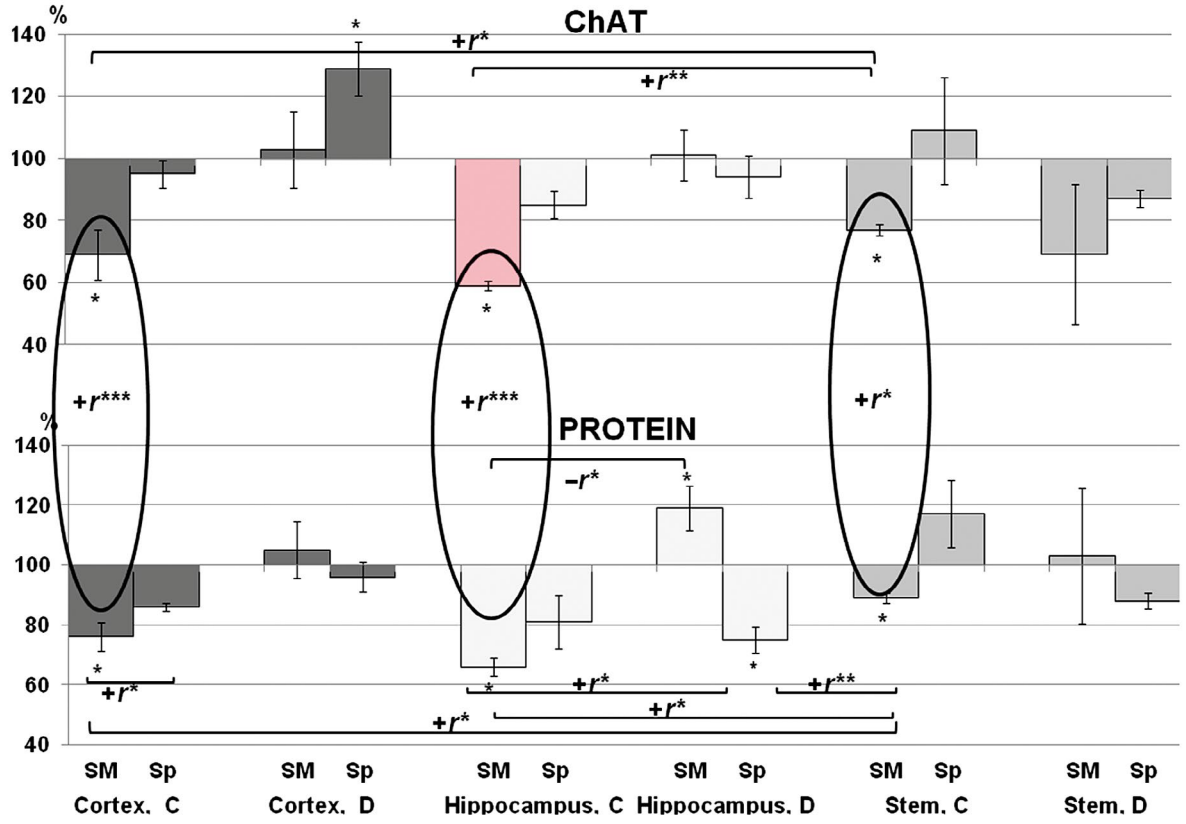

Fig. 3. Conjugacy of HBH-initiated changes in the synaptic ChAT activity and Pr content in the hippocampus, cerebral cortex, and caudal brainstem in rats with PPI < 40%. Designations. The ChAT activity and Pr content values are represented as a percentage change (mean ± SEM%) relative to the values in the corresponding control subgroup, which were taken as 100%. Cortex, the cerebral cortex. Stem, the caudal brainstem. C and D, the fractions of light and heavy synaptosomes, respectively, as in Figure 1. SM, the synaptic membrane subfraction. Sp, the synaptoplasm subfraction. The SM and Sp indicators are shown in pairs according to their belonging to a synaptosome fraction. ChAT, top row, the ChAT activity. PROTEIN, bottom row, the Pr content. Accordingly, in each brain structure, changes in mChAT/mPr values are presented in SM, and changes in sChAT/ sPr values are presented in Sp. For better perception, the indicators of different brain structures (Cortex, Hippocampus, Stem) are presented in different colors (different shades of gray). In the Hippocampus, C, the SM column is highlighted in red in the 'ChAT' row, as it is a key indicator for the mechanism of hypoxic preconditioning. *, significant differences from the corresponding control subgroups, $p < 0.05$, n = 3, Fisher's exact test (FET-criterion), which for ChAT is similar to the '#' marker in Figure 1. Ovals represent a significant correlation between changes in ChAT activity and Pr content in a subfraction (an intrafractional association), Pearson's test (*r*-criterion). Horizontal brackets indicate a significant correlation of indicator changes (ChAT or Pr) between different subfractions (an interfractional and interstructural coherence) according to Pearson's test (*r*-criterion). *+r/ -r*, positive/negative correlation, respectively; *r*/ r**/ r****, $p < 0.05$/ $p < 0.02$/ $p < 0.01$, respectively; n = 6 for each sample.

Рис. 3. Сопряженность НВН-инициируемых изменений в синаптической активности ХАТ и содержании белка (Pr) в гиппокампе, коре головного мозга и каудальном стволе гоовного мозга у крыс с ПСТ< 40%. Обозначения. Изменения в активности ХАТ и содержании белка представлены в процентах (M ± м%) по отношению к значениям в соответствующих субфракциях контрольной подгруппы, принятым за 100%. Cortex – кора головного мозга. Stem – каудальный ствол головного мозга. C и D – фракции легких и тяжелых синаптосом соответственно, как на рис. 1. SM – субфракция синаптических мембран. Sp – субфракция синаптоплазмы. Индикаторы SM и Sp спарены в соответствии с их принадлежностью к фракции синаптосом. ChAT – верхний ряд, активность ХАТ. PROTEIN – нижний ряд, содержание белка. Соответственно, в каждой структуре мозга, в субфракциях SM представлены изменения значений mChAT/mPr, а в субфракциях Sp представлены изменения значений sChAT/sPr. Для лучшего восприятия показатели разных структур мозга (коры, гиппокампа, ствола) представлены разными оттенками серого. В ряду "ChAT", в гиппокампе С столбец SM выделен розовым цветом, поскольку это ключевой индикатор в механизме гипоксического прекондиционирования. * – достоверные отличия от соответствующих контрольных подгрупп, идентичны маркеру "#" на рис. 1 и 2, $p < 0.05$, n = 3, Точный Метод Фишера (ТМФ-критерий). Овалы обозначают значимую корреляцию между изменениями в активности ХАТ и содержании белка в пределах субфракции (внутрифракционная ассоциация), тест Пирсона (*r*-критерий). Горизонтальные скобки индексируют значимую корреляцию изменений биохимических показателей (активности ХАТ или содержания белка) в разных субфракциях (межфракционная и межструктурная когерентность, *r*-критерий). *+r/ -r* – положительная/отрицательная корреляция соответственно; *r*/ r**/ r**** – $p < 0.05$/ $p < 0.02$/ $p < 0.01$ соответственно; n = 6 для каждой выборки.

Table 1. Significant correlation values of HBH-initiated changes in the synaptic ChAT activity and Pr content in the hippocampus, cerebral cortex, and caudal brainstem in rats with PPI < 40% (I – III) and > 40% (IV – VI)

Таблица 1. Значения достоверных корреляций инициируемых ГБГ изменений синаптической активности ХАТ и содержания белка в гиппокампе, коре головного мозга и каудальном стволе головного мозга у крыс с ПСТ < 40% (I – III) и ПСТ > 40% (IV – VI)

I, ChAT – ChAT				
Fraction	Pirson's test/ Fraction	Hippocampus, C,SM	Hippocampus, D, Sp	Cortex, C, SM
Stem, C, SM	*r*	+0.936		+0.863
	P	P < 0.02		P < 0.05
II, Pr – Pr				
Fraction	Pirson's test/ Fraction	Hippocampus, C, SM	Hippocampus, D, Sp	Cortex, C, SM
Stem, C, SM	*r*	+0.880	+0.956	+0.878
	P	P < 0.05	P < 0.02	P < 0.05
Hippocampus,D, SM	*r*	-0.823		
	P	P < 0.05		
Hippocampus,D, Sp	*r*	+0.867		
	P	P < 0.05		
Cortex, C Sp	*r*			+0.895
	P			P < 0.02
III, ChAT - Pr				
Fraction	Pirson's test/ Fraction	Stem, C, SM, Pr	Hippocampus, C, SM, Pr	Cortex, C, SM, Pr
Stem, C, SM, ChAT	*r*	+0.911		
	P	P < 0.02		
Hippocampus, C, SM, ChAT	*r*		+0.977	
	P		P < 0.01	
Cortex,C, SM, ChAT	*r*			+0.972
	P			P < 0.01
IV, ChAT - ChAT				
Fraction	Pirson's test/ Fraction	Hippocampus, C, SM	Hippocampus, C, Sp	Hippocampus, D, SM
Cortex, D, SM	*r*	+0.898		
	p	P < 0.02		
Cortex, D, Sp	*r*			-0.960
	P			P < 0.01
Stem, C, Sp	*r*		+0.948	
	P		P < 0.01	
Stem, D, SM	*r*		-0.968	
	P		P < 0.01	

V, Pr - Pr				
Fraction	Pirson's test/ Fraction	Hippocampus, C, SM	Hippocampus, C, Sp	Hippocampus, D, SM
Stem, C, Sp	*r*			-0.878
	P			P < 0.05
VI, ChAT – Pr				
Fraction	Pirson's test/ Fraction	Stem, C Sp	Hippocampus, C, Sp	Hippocampus, D, SM
Stem, C, Sp	*r*	+0.866		
	P	P < 0.05		

Designations. The table includes only samples with significant ChAT–ChAT, Pr-Pr and ChAT-Pr correlations presented in Fig. 3 and 4. The designations are the same as in Figures: Cortex, the cerebral cortex; Stem, the caudal brainstem; C and D, the fractions of light and heavy synaptosomes, respectively; SM, the synaptic membrane subfraction; Sp, the synaptoplasm subfraction; ChAT, the ChAT activity; Pr, the protein content. Pearson's test (*r*-criterion), n = 6 for each sample.
Обозначения. В таблицу включены значения только достоверных корреляций ХАТ-ХАТ, белок-белок и ХАТ-белок, представленные на рис. 3 и 4. Обозначения как и на рисунках: Cortex – кора головного мозга; Stem – каудальный ствол головного мозга; C и D – фракции легких и тяжелых синаптосом соответственно; SM – субфракция синаптических мембран; Sp – субфракция синаптоплазмы; ChAT – активность ХАТ; Pr – содержание белка. Метод Пирсона (r-критерий), n = 6 для каждой выборки.

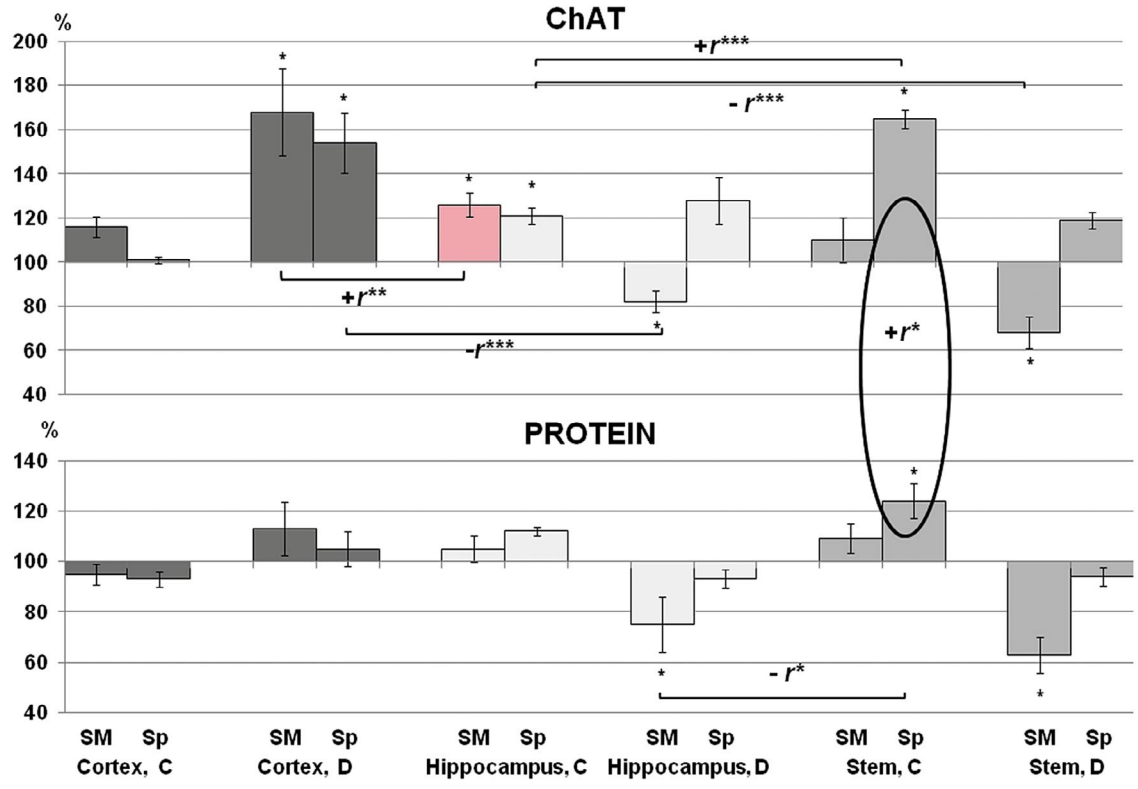

Fig. 4. Conjugacy of HBH-initiated changes in the synaptic ChAT activity and Pr content in the hippocampus, cerebral cortex, and caudal brainstem in rats with PPI > 40%. The designations are the same as those in Figure 2.
Рис. 4. Сопряженность ГБГ-инициируемых изменений в синаптической активности ХАТ и содержании белка в гиппокампе, коре головного мозга и каудальном стволе головного мозга у крыс с ПСТ > 40%. Обозначения как на рис. 3.

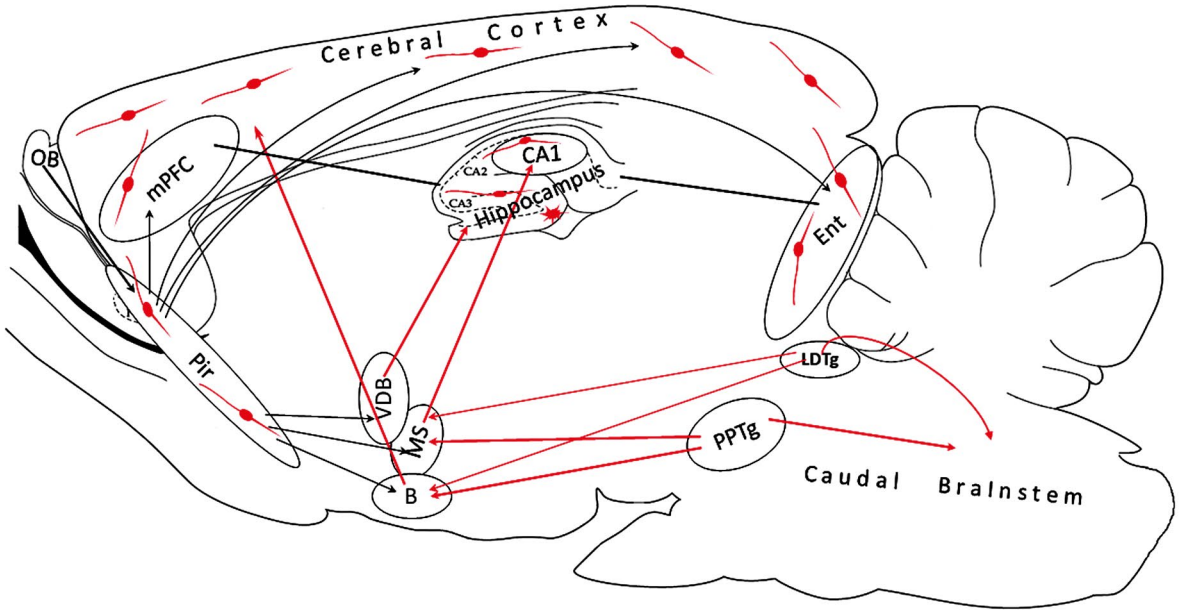

Fig. 5. Scheme of the sources of cholinergic influences in the cerebral cortex and hippocampus, as well as components of neural networks of hypoxic preconditioning. The scheme is based on the Rat Brain Atlas by Paxinos and Watson (Paxinos, Watson, 1998) and later data on the stereotaxic coordinates of the prefrontal cortex (Sampath et al., 2017; Wirt, Hyman, 2017). Designations. B, nucleus basalis magnocellularis. CA1, CA2, CA3, fields of the hippocampus. Caudal Brainstem, medulla oblongata + pons Varolii. Ent, entorhinal cortex. LDTg, laterodorsal tegmental nucleus. LC, locus coeruleus. MS, medial septal nucleus. mPFC, medial prefrontal cortex. OB, olfactory bulb. Pir, piriform cortex. PPTg, pedunculopontine tegmental nucleus. VDB, nucleus of the vertical limb of the diagonal band. Red ovals with short processes in the cerebral cortex and hippocampus, cholinergic interneurons (predominantly bipolar neurons). Red lines, cholinergic projections from the nuclei of the forebrain and tegmental nuclei of the midbrain. Black lines, projections of other neuromediation (most often glutamatergic). The arrows indicate a direction of projections to a target structure. Where known, a line thickness reflects the relative power of single-color projections. The scheme shows only the brain structures and connecting fibers that are mentioned in the text.

Рис. 5. Схема источников холинергических влияний в неокортексе и гиппокампе, а также компонентов нейронных сетей гипоксического прекондиционирования. Схема основана на Атласе мозга крысы Паксиноса и Уотсона (Paxinos, Watson, 1998) и более поздних данных о стереотаксических координатах префронтальной коры (Sampath et al., 2017; Wirt, Hyman, 2017). Обозначения. B – базальное крупноклеточное ядро. CA1, CA2, CA3 – поля гиппокампа. Caudal Brainstem – каудальный ствол головного мозга (продолговатый мозг + Варолиев мост). Cerebral Cortex – кора головного мозга. Ent – энторинальная кора. Hippocampus – гиппокамп. LDTg – латеродорсальное тегментальное ядро. MS – медиальное ядро перегородки. mPFC – медиальная префронтальная кора. OB – обонятельная луковица. Pir – грушевидная кора. PPTg – педункулопонтинное тегментальное ядро. VDB – ядро вертикального лимба диагональной связки. Красные овалы с короткими отростками в коре головного мозга и гиппокампе – холинергические интернейроны (преимущественно биполярные). Красные линии – холинергические проекции из ядер переднего мозга и тегментальных ядер среднего мозга. Черные линии – проекции других нейромедиаторов (чаще всего глутаматергических). Стрелки указывают направление проекций на целевую структуру. Если известно, толщина линии отражает относительную мощность одноцветных проекций. На схеме показаны только те структуры мозга и соединительные волокна, которые упомянуты в тексте.

involved in the generation of theta rhythm in the preconditioning mechanism of HBH.

Analysis of the Composition of the Neuronal Network of Hypoxic Preconditioning in Rats with PPI < 40% (Figure 3)

Cholinergic Presynaptic Components of the Neuronal Network

In the subgroup of rats with PPI < 40%, HBH initiated a decrease in mChAT activity in the light fractions of the hippocampus, cortex and caudal brainstem. This indicated the inhibition of neurotransmitter function in the cholinergic projective neurons of the hippocampus and cortex, as well as in the population of the cholinergic synaptic pool of the caudal brainstem. The decrease in mChAT activity in the caudal brainstem was positively correlated with a decrease in mChAT activity in both the hippocampus and cortex. There was no correlation between the cortex and hippocampus. Therefore we concluded that the reaction in the caudal brainstem was primary, and its effects

extended to the cholinergic projective neurons of the forebrain nuclei of the cortex and hippocampus.

The synaptic response in all three structures – through a decrease in mChAT activity – was correlated with a decrease in mPr content in the corresponding fractions. The decrease in both biochemical parameters occurred conjugately (positive intrafractional correlations mChAT–mPr). Moreover, the mPr content showed the same correlations of the caudal brainstem with the hippocampus and cortex as those for mChAT.

The density of the cholinergic fibers of projective cholinergic laterodorsal (LDTg) and pedunculopontine (PPTg) nuclei from the middle-brain tegmentum is much more powerful than that of any other network of cholinergic fibers in the caudal brainstem (Woolf, Butcher, 1989; Jones, 1990). For both tegmental nuclei, the synaptic manner of transmitting cholinergic signals was characteristic and size of these synapses (medium and small) corresponded to the presynapses of the light fraction of synaptosomes (Bautista et al., 2010). Thus, it is likely that a reaction of projective presynapses from LDTg and PPTg was manifested in the fraction of light synaptosomes of the caudal brainstem.

PPTg and LDTg are the main relay nuclei between the cortical cholinergic projective neurons and brainstem formations (Semba et al., 1989). This signal transmission scheme can provide an interstructural association that explains the coherence of the cholinergic reaction in both the cerebral cortex and hippocampus with the cholinergic reaction in the caudal brain stem (Figure 5). However, there is a lack of association between the cortex and hippocampus in this cholinergic response. Therefore, it is possible that another source of innervation of the cholinergic nuclei of the forebrain is also involved in the preconditioning mechanism.

Noncholinergic Presynaptic Components of the Neuronal Network

The study of synaptic proteins also revealed a reaction to HBH of a noncholinergic nature in the presynapses in the heavy fraction of hippocampal synaptosomes. The increase in mPr and the decrease in sPr content were not correlated with each other, but both indicators were correlated with the mPr content in the light fraction of the hippocampus. In addition, the sPr content was correlated with the mPr content of the synaptic presynapses in the light fraction of the caudal brainstem. Thus, these correlations reflect the involvement of the noncholinergic synaptic pool of the hippocampus in the hypoxic preconditioning neural network.

Note that in the heavy fractions of synaptosomes, GABAergic and glutamatergic presynapses dominate (see the review in (Zakharova et al., 2018b)). In the hippocampus, GABAergic and glutamatergic neurons are both mandatory components of the theta oscillation network and targets of projected cholinergic influences (Müller, Remy, 2018; Zinchenko et al., 2020; Gu, Yakel, 2022).

Analysis of the Composition of the Neuronal Network of Hypoxic Preconditioning in Rats with PPI > 40% (Figure 4)

Cholinergic Presynaptic Components of the Neuronal Network

In the subgroup of rats with PPI > 40%, the activation of mChAT in the light fraction of hippocampal synaptosomes was associated with the activation of mChAT in the heavy fraction of the cerebral cortex. There were no correlations of the mChAT activity in this fraction with the synaptic populations of the caudal brainstem.

Unlike mChAT, the activation of sChAT in the same light fraction of the hippocampus was associated with the activation of sChAT in the light fraction of synaptosomes and a negative correlation with the decrease in mChAT activity in the heavy fraction of the caudal brainstem. However, this reorganization led to intersubgroup alignment in ChAT activity in both the hippocampus and caudal brainstem. Therefore, this did not meet the criterion for the involvement of corresponding cholinergic synaptic populations in the performance of hypoxic preconditioning.

The lack of coherence of key neurons with the ascending airways in the HBH mechanism became possible to explain by scientific research over the past 20 years on the existence of breathing-sensitive neurons in the cerebral cortex.

It was found that neurons in the nasal olfactory epithelium respond to mechanical stimuli, including airflow pressure (Connelly et al., 2015; Girin et al., 2021; Juventin et al., 2023) and an odorless airflow (Carey et al., 2009; Phillips et al., 2012; Vaaga, Westbrook, 2016, Salimi et al., 2023). Moreover, nasal respiratory rhythms have been shown to modulate cortical rhythmic activity (Fontanini et al., 2003; Connelly et al., 2015; Lockmann et al., 2016; Vaaga, Westbrook, 2016; Heck et al., 2019; Girin et al., 2021; Sheriff et al., 2021, Salimi et al., 2023), and it has been shown that cortical rhythms disappear after tracheotomy and they reappear by artificially passing

air through the nose (Fontanini et al., 2003; Lockmann et al., 2016).

It is especially important that that several years ago, an atypical class of sensory neurons, the type B cells, were identified in the main olfactory epithelium. These type B cells are not sensitive to atmospheric oxygen (pO_2 is 159 mm Hg) and are activated by low O_2, starting from pO_2 is 138 mm Hg (Bleymehl et al., 2016; Koike et al., 2021). Such data allow us to assume the existence of own cortical regulatory mechanism under the conditions of adaptive hypoxia.

The presynapses of cholinergic interneurons are concentrated in the heavy fraction of synaptosomes of the cerebral cortex. At the same time, the anatomical connections of the olfactory brain with the cortical regions and hippocampus are well known. In the olfactory brain, the piriform area is the main switching link of sensory information (Sheriff et al., 2021). Direct connections of the piriform area with the hippocampus and cortex have been shown, including the prefrontal and entorhinal cortical areas, and the primacy of the signal in the piriform cortex in relation to the hippocampus and entorhinal cortex has been traced (de Curtis et al., 2019; Sheriff et al., 2021; Zhou et al., 2021), as well as that with forebrain subcortical cholinergic nuclei, which are projected both in the hippocampus and cortex (Biagioni et al., 2019).

Therefore, it is likely that the piriform area is the structure that transmits respiratory stimuli from the olfactory epithelium to the cholinergic interneurons of the cortex and to the corresponding cholinergic subcortical nuclei that innervate the hippocampus (Figure 5).

In our study, both mChAT and sChAT were activated in the heavy fraction of the cortex. There were no correlations between these indicators. Therefore, we believe that the observed changes occurred in the presynapses of different populations of interneurons.

Noncholinergic Presynaptic Components of the Neuronal Network

In the heavy fraction of synaptosomes in the hippocampus, there was a decrease in the mPr content in presynapses of a noncholinergic nature. The negative correlation with the increase in the sPr content in the fraction of light synaptosomes of the caudal brainstem indicated the involvement of this population of noncholinergic presynapses (GABA- or glutamatergic) in the same neural network as that of the corresponding cholinergic populations of the caudal brainstem and hippocampus.

Physiological Significance of the Brain's Cholinergic Response to HBH

In this experiment, after HBH, the lower limit of resistance to SHBH was 5 min 29 s for the rats with PPI > 40%, while for the rats with PPI < 40%, it was 8 min 51 s.

In all of our experiments, for the rats with PPI > 40%, this lower limit was 4 min 20 s, while for the rats with PPI < 40%, it corresponded to the above (Dudchenko et al., 2014; Zakharova et al., 2018a, 2018b, 2020). The network differences in the implementation of hypoxic preconditioning in the rats with PPI values of < 40% or > 40% may be critical for the efficiency of HBH.

Increase of resistance to severe hypoxia in these subgroups of rats as a result of multidirectional functional changes in the same population of neurons is a poorly understood problem. Apparently, we first formulated this problem in this and our previous research (Zakharova et al., 2020). In the previous study, we hypothesized that the differential changes in ChAT activity in the subgroups of animals with PPI less than or greater than 40% may be a biochemical equivalent of theta filtering mechanism. And also we hypothesized that a physiological cause of these differences may be the different ways of its regulation. The second assumption is supported by the results of this study, which suggest radically different ways of its regulation in these subgroups of animals.

ChAT activity is the specific indicator for monitoring the functional state of cholinergic neurons and has become increasingly in demand over the years. This has been demonstrated both in the studies of ChAT activity and registration of EEG patterns in the hippocampus (Monmaur et al., 1984), and in experimental impairment of nervous functions or at early stages of neurodegenerative disorders in animals and humans (Dunbar et al., 1993; Zakharova, Dudchenko, 2014; Bagwe, Sathaye, 2022; Kirstein et al., 2022; AlQot, Rylett, 2023).

The activation of synaptic mChAT reflects, as a rule, the activation of synaptic cholinergic function (see the review in (Zakharova, Dudchenko, 2014)). It has been repeatedly shown that the activation of cholinergic projections of the hippocampus is necessary for the generation of theta rhythm (Müller, Remy, 2018; Ma et al., 2020; Gu, Yakel, 2022). Thus, our data in rats with PPI > 40% are consistent with the literature.

On the contrary, in rats with PPI < 40%, a conjugated synaptic reaction in all three structures occurred through a decrease in mChAT activity. A similar re-

sponse to HBH of synaptic protein in the same subfractions reinforces these data. This, at first glance, contradicts the ideas about the role of the cholinergic mechanisms of the hippocampal theta rhythm in the rats with PPI > 40%, but this is a question that requires careful investigation. Thus, a number of studies have data that the interaction of cholinergic projections with hippocampal interneurons contributes to an adaptation of the theta rhythm to a current form of behavior (Gu, Yakel, 2022). In particular, the authors of this study provided data on the potentiation of the theta rhythm after cholinergic blockade.

The equalization of ChAT activity in response to HBH in the cerebral cortex and caudal brainstem may indicate the completion of the phase of perception and integration during the dominance of hippocampal phase of preconditioning. This "leveling" may reflect the filtering inherent in the theta rhythm, which provides insensitivity to stimuli from other modalities.

We also attributed the mChAT inhibition in the heavy fraction of hippocampal synaptosomes in the subgroup of rats with PPI > 40% to the filtration mechanism. This was the only fraction in which HBH did not even out but rather further deepened the intergroup differences. The cholinergic presynapses in this fraction are necessary for successful consolidation of early spatial memory (Zakharova et al., 2022).

These data could be consistent with our pharmacological experiments. Alpha7 subtype of nAChRs is recognized as procognitive receptors, the elimination of which blocks the possibility of memory consolidation during learning (Lykhmus et al., 2020; Sadigh-Eteghad et al.,2020; Shenkarev et al., 2020; Cheng et al., 2021). In our experiments, selective agonist of receptors of this subtype PNU abolished the effect of its DMSO solvent on HBH and, at high concentrations, suppressed the preconditioning effect of HBH in rats with PPI > 40% under IP and intrahippocampal administration (Zakharova et al., 2020, 2021).

It is also known that alpha7 nAChRs is involved in the hippocampal theta rhythm (Hummos, Nair, 2017; Gu, Yakel, 2022). Therefore it seems obvious that the theta rhythm is realized through different neural networks and various neurotransmitter receptors depending on the source of significant sensory stimulation and from PPI.

CONCLUSIONS

1. The first data on the central cholinergic components of neural networks in the mechanism of hypoxic preconditioning are presented.

2. Differences in the composition of hypoxic preconditioning network were revealed in rats with PPI values <40% and >40%. The neural network included cholinergic synapses of the hippocampus, caudal brainstem and cerebral cortex in rats with low PPI and only of the hippocampus and cortex in rats with high PPI.

3. A working hypothesis is substantiated that in the subgroups of rats with different PPI levels, hypoxic preconditioning is realized in the hippocampus through neural networks that include topographically different sensory inputs, namely respiratory neurons of the brainstem in rats with low PPI and respiratory neurons of the olfactory epithelium in rats with high PPI.

4. We hope that this direction of research will help to best realize the innate individual abilities of the body while optimizing personalized modes of adaptation to hypoxia.

REFERENCES

Akopyan N.S., Baklavadzhyan O.G., Karapetyan M.A. Effects of acute hypoxia on the EEG and impulse activity of the neurons of variousconelly brain structures in rats. Neurosci. Behav. Physiol. 1984. 14 (5): 405–411.

AlQot H.E., Rylett R.J. A novel transgenic mouse model expressing primate-specific nuclear choline acetyltransferase: insights into potential cholinergic vulnerability. *Sci Rep*. 2023. 13 (1): 3037.

Ando S., Komiyama T., Sudo M., Higaki Y., Ishida K., Costello J.T., Katayama K. The interactive effects of acute exercise and hypoxia on cognitive performance: A narrative review. Scand. J. Med. Sci. Sports. 2020. 30 (3): 384–398.

Appelbaum L.G., Shenasa M.A., Stolz L., Daskalakis Z. Synaptic plasticity and mental health: methods, challenges and opportunities. Neuropsychopharmacology. 2022. 48: 113–120.

Ashhad S., Kam K., Del Negro C.A., Feldman J.L. Breathing Rhythm and Pattern and Their Influence on Emotion. Annu. Rev. Neurosci. 2022. 45: 223–247.

Bagwe P., Sathaye S. Significance of Choline Acetyltransferase Enzyme in Tackling Neurodegenerative Diseases. Current Molecular Biology Reports. 2022. 8: 9–22.

Bautista T.G., Sun Q.J., Zhao W.J., Pilowsky P.M. Cholinergic inputs to laryngeal motoneurons functionally identified in vivo in rat: A combined electrophysiological and microscopic study. J. Comp. Neurol. 2010. 518: 4903–4916.

Biagioni F., Gaglione A., Giorgi F.S., Bucci D., Moyanova S., De. Fusco A., Madonna, M., Fornai F. Degeneration of cholinergic basal forebrain nuclei after focally evoked status epilepticus. Neurobiol. Dis. 2019. 121: 76–94.

Bleymehl K., Pérez-Gómez A., Omura M., Moreno-Pérez A., Macías D., Bai Z., Johnson R.S., Leinders-Zufall T.,

Zufall F., Mombaerts P.A. Sensor for Low Environmental Oxygen in the Mouse Main Olfactory Epithelium. Neuron. 2016. 92: 1196–1203.

Carey R.M., Verhagen J.V., Wesson D.W., Pírez N., Wachowiak M. Temporal structure of receptor neuron input to the olfactory bulb imaged in behaving rats. J. Neurophysiol. 2009. 101: 1073–1088.

Cheng Q., Lamb P., Stevanovic K., Bernstein B.J., Fry S.A., Cushman J.D., Yakel J.L. Differential signalling induced by **α7** nicotinic acetylcholine receptors in hippocampal dentate gyrus in vitro and in vivo. J. Physiol. 2021. 599 (20): 4687–4704.

Connelly T., Yu .Y., Grosmaitre X., Wang J., Santarelli L.C., Savigner A., Qiao X., Wang Z., Storm D.R., Ma. M. G protein-coupled odorant receptors underlie mechanosensitivity in mammalian olfactory sensory neurons. Proc. Natl. Acad. Sci. U S A. 2015. 112: 590–595.

Das M., Das D.K. Molecular Mechanism of Preconditioning. IUBMB Life. 2008. 60: 199–203.

de Curtis M., Uva L., Lévesque M., Biella G., Avoli M. Piriform cortex ictogenicity in vitro. Exp. Neurol. 2019. 321: 113014.

Dudchenko A.M., Zakharova E.I., Storozheva Z.I. Method for Predicting the Limit of Resistance of Animals to Severe Hypoxia after Hypoxic Preconditioning. RF Patent 2571603. 4 July 2014.

Dunbar G.L., Rylett R.J., Schmidt B.M., Sinclair R.C., Williams L.R. Hippocampal choline acetyltransferase activity correlates with spatial learning in aged rats. Brain Res. 1993. 604 (1–2): 266–272.

Fonnum F. Radiochemical microassays for the determination of choline acetyltransferase and acetylcholinesterase activities. Biochem. J. 1969. 115: 465–472.

Fontanini A., Spano P., Bower J.M. Ketamine-Xylazine-induced slow (< 1.5 Hz) oscillations in the rat piriform (olfactory) cortex are functionally correlated with respiration. J. Neurosci. 2003. 23: 7993–8001.

Gavrilova S.A., Samojlenkova N.S., Pirogov Yu.A., Khudoerkov R.M., Koshelev V.B. Neuroprotective effect of hypoxic preconditioning in the rat brain with focal ischemia. Pathogenesis. 2008. 6 (3): 13–17. In Russian

Girin B., Juventin M., Garcia S., Lefèvre L., Amat C., Fourcaud-Trocmé N., Buonviso N. The deep and slow breathing characterizing rest favors brain respiratory-drive. Sci. Rep. 2021. 11 (1): 7044.

Gu .Z., Yakel J.L. Cholinergic Regulation of Hippocampal Theta Rhythm. Biomedicines. 2022. 10: 745.

Heck D.H., Kozma R., Kay L.M. The rhythm of memory: How breathing shapes memory function. J. Neurophysiol. 2019. 122: 563–571.

Hummos A., Nair S.S. An integrative model of the intrinsic hippocampal theta rhythm. PLoS ONE. 2017. 12: e0182648.

Jones B.E. Immunohistochemical study of choline acetyltransferase immunoreactive processes and cells innervating the pontomedullary reticular formation in the rat. J. Comp. Neurol. 1990. 295: 485–514.

Juventin M., Ghibaudo V., Granget J., Amat C., Courtiol E., Buonviso N. Respiratory influence on brain dynamics: the preponderant role of the nasal pathway and deep slow regime. Pflugers Arch. 2023. 475 (1): 23–35.

Karalis N., Sirota A. Breathing coordinates cortico-hippocampal dynamics in mice during offline states. Nat. Commun. 2022. 13: 467.

Kirstein M., Cambrils A., Segarra A., Melero A., Varea E. Cholinergic Senescence in the Ts65Dn Mouse Model for Down Syndrome. Neurochem Res. 2022. 47 (10), 3076–3092.

Kitchigina V.F. Mechanisms of the regularion and the functional significance of the Theta-Rhytm. Roles of serotonergic and noradrenergic systems. Zh. Vyssh. Nerv. Deiat. 2004. 54: 101–119. In Russian

Kobzar A.I. Applied Mathematical Statistics. For Engineers and Scientists. Moscow: FIZMATLIT, 2006. 816 p. In Russian

Koike K., Yoo S.J., Bleymehl K., Omura M., Zapiec B., Pyrski M. et al. Danger perception and stress response through an olfactory sensor for the bacterial metabolite hydrogen sulfide. Neuron. 2021. 109 (15): 2469–2484.e7.

Lara-González E., Padilla-Orozco M., Fuentes-Serrano A., Bargas J., Duhne M. Translational neuronal ensembles: Neuronal microcircuits in psychology, physiology, pharmacology and pathology. Front. Syst. Neurosci. 2022. 16: 979680.

Liu H., Shi R., Liao R., Liu Y., Che J., Bai Z., Cheng N., Ma H. Machine Learning Based on Event-Related EEG of Sustained Attention Differentiates Adults with Chronic High-Altitude Exposure from Healthy Controls**.** Brain Sci. 2022 12 (12):1677.

Lockmann A.L., Laplagne D.A., Leão R.N., Tort A.B. A Respiration-Coupled Rhythm in the Rat Hippocampus Independent of Theta and Slow Oscillations. J. Neurosci. 2016. 36: 5338–5352.

Lowry O.H., Rosenbrough N.J., Farr A.L., Randall R.J. Protein measurement with the Folin phenol reagent. Biol. Chem. 1959. 193: 265–275.

Lukyanova L.D., Germanova E.L., Kopaladze R.A. Development of resistance of an organism under various conditions of hypoxic preconditioning: role of the hypoxic period and reoxygenation. Bull. Exp. Biol. Med. 2009. 147: 400–404.

Lukyanova L.D., Germanova E.L,. Tsibina T.A., Kopaladze R.A., Dudchenko A.M. Efficiency and mechanism for different regimens of hypoxic training: The possibility of optimization of hypoxic therapy. Pathogenesis, 2008, 6: 32–36. In Russian

Lykhmus O., Kalashnyk O., Uspenska K., Horid'ko T., Kosyakova H., Komisarenko S., Skok M. Different Effects of Nicotine and N-Stearoyl-ethanolamine on Episodic Memory and Brain Mitochondria of **α7** Nicotinic Acetylcholine Receptor Knockout Mice. Biomolecules. 2020. 10 (2): 226.

Ma X., Zhang Y., Wang L., Li .N., Barkai E., Zhang X., Lin L., Xu J. The Firing of Theta State-Related Sep-

tal Cholinergic Neurons Disrupt Hippocampal Ripple Oscillations via Muscarinic Receptors. J. Neurosci. 2020. 40 (18): 3591–3603.

Maslov L.N., Lishmanov Yu.B., Emelianova T.V., Prut D.A., Kolar F., Portnichenko A.G. et al. Hypoxic Preconditioning as Novel Approach to Prophylaxis of Ischemic and Reperfusion Damage of Brain and Heart. Angiol. Sosud. Khir. 2011; 17 (3): 27–36. In Russian

Monmaur P., Fage D., M'Harzi M., Delacour J., Scatton B. Decrease in both choline acetyltransferase activity and EEG patterns in the hippocampal formation of the rat following septal macroelectrode implantation. Brain Res. 1984. 293 (1): 178–183.

Müller C., Remy S. Septo-hippocampal interaction. Cell Tissue Res. 2018. 373 (3): 565–575.

Navarrete-Opazo A., Mitchell G.S. Therapeutic potential of intermittent hypoxia: a matter of dose. Am. J. Physiol. Regul. Integr. Comp. Physiol. 2014. 307 (10): R1181–R1197.

Obermayer J., Luchicchi A., Heistek T.S., de Kloet S.F., Terra H., Bruinsma B. et al. Prefrontal cortical ChAT-VIP interneurons provide local excitation by cholinergic synaptic transmission and control attention. Nat. Commun. 2019. 10: 5280.

Paxinos G., Watson Ch. Rat Brain in Stereotaxic Coordinates, Fourth Edition, San Diego: Academic Press, 1998, 474 p.

Phillips M.E., Sachdev R.N., Willhite D.C., Shepherd G.M. Respiration drives network activity and modulates synaptic and circuit processing of lateral inhibition in the olfactory bulb. J. Neurosci. 2012. 32: 85–98.

Radhakrishnan S., Martin C.A., Dhayanithy G., Reddy M.S., Rela M., Kalkura S.N., Sellathamby S. Hypoxic Preconditioning Induces Neuronal Differentiation of Infrapatellar Fat Pad Stem Cells through Epigenetic Alteration. ACS Chem. Neurosci. 2021. 12: 704–718.

Ramadan M.Z., Ghaleb A.M., Ragab A.E. Using Electroencephalography (EEG) Power Responses to Investigate the Effects of Ambient Oxygen Content, Safety Shoe Type, and Lifting Frequency on the Worker's Activities. Biomed. Res. Int. 2020: 7956037.

Rybnikova E.A., Nalivaeva N.N., Zenko M.Y., Baranova K.A. Intermittent Hypoxic Training as an Effective Tool for Increasing the Adaptive Potential, Endurance and Working Capacity of the Brain. Front. Neurosci. 2022. 16: 941740.

Sadigh-Eteghad S., Vatandoust S.M., Mahmoudi J., Rahigh Aghsan S., Majdi A. Cotinine ameliorates memory and learning impairment in senescent mice. Brain Res. Bull. 2020. 164: 65–74.

Sampath D., Sathyanesan M., Newton S.S. Cognitive dysfunction in major depression and Alzheimer's disease is associated with hippocampal-prefrontal cortex dysconnectivity. Neuropsychiatr. Dis. Treat. 2017. 13: 1509–1519.

Salimi M., Ayene F., Parsazadegan T., Nazari M., Jamali Y., Raoufy M.R. Nasal airflow promotes default mode network activity. Respir. Physiol. Neurobiol. 2023. 307:103981.

Sawada M., Sato M. The effect of dimethyl sulfoxide on the neuronal excitability and cholinergic transmission in Aplysia ganglion cells. Ann. N. Y. Acad. Sci. 1975. 243: 337–357.

Semba K., Reiner P.B., McGeer E.G., Fibiger H.C. Brainstem projecting neurons in the rat basal forebrain: Neurochemical, topographical, and physiological distinctions from cortically projecting cholinergic neurons. Brain Res. Bull. 1989. 22: 501–509.

Shenkarev Z.O., Shulepko M.A., Bychkov M.L., Kulbatskii D.S., Shlepova O.V., Vasilyeva N.A. et al. Water-soluble variant of human Lynx1 positively modulates synaptic plasticity and ameliorates cognitive impairment associated with **α7**–nAChR dysfunction. J. Neurochem. 2020. 155 (1):45–61.

Sheriff A., Pandolfi G., Nguyen V.S., Kay L.M. Long-Range Respiratory and Theta Oscillation Networks Depend on Spatial Sensory Context. J. Neurosci. 2021. 41: 9957–9970.

Vaaga C.E., Westbrook G.L. Parallel processing of afferent olfactory sensory information. J. Physiol. 2016. 594: 6715–6732.

Wirt R.A., Hyman J.M. Integrating Spatial Working Memory and Remote Memory: Interactions between the Medial Prefrontal Cortex and Hippocampus. Brain Sci. 2017. 7 (4): 43.

Wood G.K., Tomasiewicz H., Rutishauser U., Magnuson T., Quirion R., Rochford J., Srivastava L.K. NCAM-180 knockout mice display increased lateral ventricle size and reduced prepulse inhibition of startle. Neuroreport. 1998. 9: 461–4666.

Woolf N.J., Butcher L.L. Cholinergic systems in the rat brain: IV. Descending projections of the pontomesencephalic tegmentum. Brain Res. Bull. 1989. 23: 519–540.

Yang Y., Gritton H., Sarter M., Aton S.J., Booth V., Zochowski M. Theta-gamma coupling emerges from spatially heterogeneous cholinergic neuromodulation. PLoS Comput. Biol. 2021. 17: e1009235.

Yoder R.M., Pang K.C. Involvement of GABAergic and cholinergic medial septal neurons in hippocampal theta rhythm. Hippocampus. 2005. 15: 381–392.

Zakharova E.I., Dudchenko A.M. Hypoxic Preconditioning Eliminates Differences in the Innate Resistance of Rats to Severe Hypoxia. Journal of Biomedical Science and Engineering. 2016. 9: 563–575.

Zakharova E.I., Dudchenko A.M. Synaptic soluble and membrane-bound choline acetyltransferase as a marker of cholinergic function in vitro and in vivo. Neurochemistry. Ed. Heinbockel T. Rijeka: InTechOpen, 2014. 5: 143–178 pp.

Zakharova E.I., Dudchenko A.M., Germanova E.L. Effects of preconditioning on the resistance to acute hypobaric hypoxia and their correction with selective antagonists

of nicotinic receptors. Bull. Exp. Biol. Med. 2011. 151 (2): 179–182.

Zakharova E.I., Proshin A.T., Monakov M.Y., Dudchenko A.M. Cholinergic Internal and Projection Systems of Hippocampus and Neocortex Critical for Early Spatial Memory Consolidation in Normal and Chronic Cerebral Hypoperfusion Conditions in Rats with Different Abilities to Consolidation: The Role of Cholinergic Interneurons of the Hippocampus. Biomedicines. 2022. 10: 1532.

Zakharova E.I., Proshin A.T., Monakov M.Y., Dudchenko A.M. Effect of Intrahippocampal Administration of α7 Subtype Nicotinic Receptor Agonist PNU-282987 and Its Solvent Dimethyl Sulfoxide on the Efficiency of Hypoxic Preconditioning in Rats. Molecules. 2021. 26: 7387.

Zakharova E.I., Storozheva E.I., Proshin A.T., Monakov M.Y., Dudchenko A.M. The Acoustic Sensorimotor Gating Predicts the Efficiency of Hypoxic Preconditioning. Participation of the Cholinergic System in This Phenomenon. J. Biomed. Sci. Eng. 2018a. 11: 10–25.

Zakharova E.I., Storozheva Z.I., Proshin A.T., Monakov M.Y., Dudchenko A.M. Hypoxic Preconditioning: The multiplicity of central neurotransmitter mechanisms and method of predicting its efficiency. Hypoxia and Anoxia. Eds. Das K.K., Biradar M.S., London: InTechOPEN, 2018b. 6: 95–131 pp.

Zakharova E.I., Storozheva Z.I., Proshin A.T., Monakov M.Y., Dudchenko A.M. Opposite Pathways of Cholinergic Mechanisms of Hypoxic Preconditioning in the Hippocampus: Participation of Nicotinic α7 Receptors and Their Association with the Baseline Level of Startle Prepulse Inhibition. Brain Sci. 2020. 11: 12.

*Zenko M.Y., Rybnikova E.A.*Cross Adaptation: from F.Z. Meerson to the Modern State of the Problem. Part 1. Adaptation, Cross-Adaptation and Cross-Sensitization. Usp. Fiziol. Nauk. 2019. 50 (4): 3–13. In Russian

Zhou G., Olofsson J.K., Koubeissi M.Z., Menelaou G., Rosenow, J., Schuele S.U. et al. Human hippocampal connectivity is stronger in olfaction than other sensory systems. Prog. Neurobiol. 2021. 201: 102027.

Zinchenko V.P., Gaidin S.G., Teplov I.Yu., Kosenkov A.M., Sergeev A.I., Dolgacheva L.P., Tuleuhanov S.T. Visualization, Properties, and Functions of GABAergic Hippocampal Neurons Containing Calcium-Permeable Kainate and AMPA Receptors. Biochemistry (Moscow), Supplement Series A: Membrane and Cell Biology. 2020. 14: 44–53.

ГИПОКСИЧЕСКОЕ ПРЕКОНДИЦИОНИРОВАНИЕ У КРЫС С НИЗКИМ И ВЫСОКИМ ПРЕДСТИМУЛЬНЫМ ТОРМОЖЕНИЕМ АКУСТИЧЕСКОГО ВЗДРАГИВАНИЯ ОСУЩЕСТВЛЯЕТСЯ ЧЕРЕЗ ТОПОГРАФИЧЕСКИ РАЗЛИЧНЫЕ СЕНСОРНЫЕ ВХОДЫ. РАБОЧАЯ ГИПОТЕЗА

Е. И. Захарова[1,*], З. И. Сторожева[2], А. Т. Прошин[2], М. Ю. Монаков[1], А. М. Дудченко[1]

[1] ФГБНУ Институт общей патологии и патофизиологии, Москва, Россия

[2] ФГБНУ ФИЦ оригинальных и перспективных биомедицинских и фармацевтических технологий, Москва, Россия

** e-mail: zakharova-ei@yandex.ru*

Нейромедиаторные и сетевые механизмы гипоксического прекондиционирования практически не изучены. Ранее на крысах мы выявили ключевую роль гиппокампа и его холинергических проекций в прекондиционирующем механизме однократной умеренной гипобарической гипоксии (ГБГ) благодаря ассоциации между эффективностью ГБГ и величиной предстимульного торможения в акустической стартл-реакции (ПСТ). В настоящем исследовании представлены первые данные о ПСТ-зависимых нейрональных сетях гипоксического прекондиционирования и их холинергических компонентах. Для корреляционного анализа использовалась активность синаптической холинацетилтрансферазы (ХАТ), индикатора холинергической функции как показатель реакции на ГБГ в гиппокампе, коре головного мозга и каудальном отделе ствола головного мозга у животных с различным уровнем ПСТ. У крыс с ПСТ < 40% активность ХАТ коррелировала в гиппокампе, коре и каудальном отделе ствола мозга, а у крыс с ПСТ > 40% – в гиппокампе и коре головного мозга. Предполагается, что ГБГ реализуется через топографически различные сенсорные входы, а именно через дыхательные нейроны ствола мозга у крыс с низким уровнем ПСТ и дыхательные нейроны обонятельного эпителия у крыс с высоким уровнем ПСТ.

Ключевые слова: гипоксическое прекондиционирование; нейронные (биологические) сети; ГБГ; ПСТ; гиппокамп; кора головного мозга; каудальный ствол головного мозга; холинергические проекцинные нейроны из ядер переднего мозга и интернейроны; “легкие” и “тяжелые” синаптосомы; синаптическая мембраносвязанная и водорастворимая ХАТ